Supporting Information

Modified graphene foam as a high-performance catalyst for oxygen reduction reaction

Malgorzata Skorupska [a,*], Anna Ilnicka [a] and Jerzy P. Lukaszewicz [a,b]

[a] Faculty of Chemistry, Nicolaus Copernicus University in Torun, Gagarina 7, 87-100 Torun, Poland

[b] Centre for Modern Interdisciplinary Technologies, Nicolaus Copernicus University in Torun, Wilenska 4, 87-100 Torun, Poland

[*] Correspondence: m.skorupska@doktorant.umk.pl (M.S.); Tel.: +48 506841438

Materials and methods

Synthesis of N-doped graphene-foams

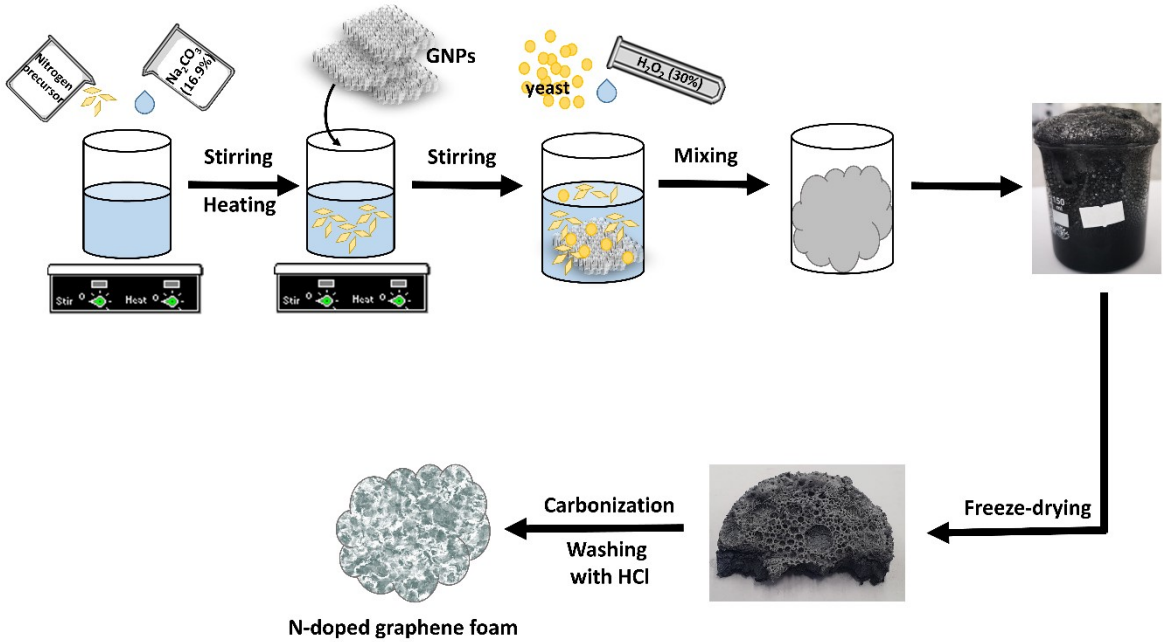

Scheme S1. Synthesis stages of N-doped graphene foams with the photograph of materials before and after freeze-drying.

Physicochemical characterization

Various methods were used for a detailed characterization of the physico-chemical properties of the samples.. A high-resolution transmission electron microscope (HRTEM FEI Tecnai F20 X-Twin, Brno, the Czech Republic) was used to characterize the structure. Raman spectra were obtained using a Raman spectrometer with 532 nm laser excitation (microscope InVia Renishaw, Renishaw Company, Gloucestershire, Great Britain). Low-pressure nitrogen adsorption was measured at 77 K using an automatic volumetric analyser (ASAP 2020 Plus, Micromeritics, Norcross, USA). The SSA was calculated using the Brunauer-Emmett-Teller (BET) equation, the pore distribution was determined by two-dimensional non-localised density functional theory (2D-NLDFT), the micropore volume (V_{mi}) was determined by t-plot

method, the total volume (V_t) was determined at the maximum relative pressure of p/p_0, the mesopore volume (V_{me}) was calculated by subtracting the volume of micropores from total pore volume. The elemental composition was used to determine the weight percentage of nitrogen, carbon, and hydrogen. The elemental analysis was carried out using a combustion analyser (Vario MACRO CHN, Elementar Analysensysteme GmbH, Germany). To determine the type and concentration of functional groups, the X-ray photoelectron spectroscopy (XPS) measurements were carried out with VG Scientific ESCALAB-210 analyzer (Japan); the excitation source was Al Ka ray (1486.6 eV).

Electrochemical measurements

The electrochemical properties were investigated using a rotating disk electrode (RDE) on an Autolab electrochemical analyzer (PGSTAT128N, the Netherlands). The electrochemical system for the oxygen reduction reaction consisted of three electrodes. The reference electrode was Ag/AgCl in 3 mol L^{-1} KCl, the counter-electrode was a platinum plate, and the working electrode was the obtained electrocatalyst applied on a glassy carbon electrode with a diameter of 3 mm and surface area equal 0.07065 cm^2. All electrodes were immersed in 0.1 mol L^{-1} KOH electrolyte. All materials were compared with commercial carbon consisting of platinum 20 wt.% (Pt/C). To apply a suitable amount of material to the glassy carbon electrode (mass loading of 0.4 mg cm^{-2}), an ink preparation of the resulting graphene foams and commercial catalyst (Pt/C) was required. 2.5 mg of carbon material was weighed and dispersed in 0.55 ml of a mixture of distilled H_2O, ethanol and Nafion (0.5 wt.% Nafion). Oxygen reduction reactions were studied by cyclic voltammetry (CV) and linear sweep voltammetry (LSV) measurements. Scan rates were 10 and 5 mV s^{-1} for CV and LSV, respectively. For the appropriate oxygen reduction reaction, 0.1 mol L^{-1} KOH was saturated with oxygen and then nitrogen before each CV and LSV measurement. Stability tests were

measured for 5 h at 0.5 V vs RHE. The number of transferred electrons involved in the oxygen reduction reaction was determined using the Koutecky-Levich (KL) equations at 0.5 V vs RHE.

Koutecky'ego-Levicha (KL) equations:

$$J^{-1} = J_L^{-1} + J_K^{-1} = (B\omega^{1/2})^{-1} + J_K^{-1} \quad (1)$$

$$B = 0.62nFC_0(D_0)^{2/3}\nu^{-1/6} \quad (2)$$

where: J is defined as the measured current density, J_L, and J_K are the limiting diffusion and kinetic current densities, respectively; ω is the angular velocity of the electrode; n is the number of electron transfer involved in the oxygen reduction reaction; F is assigned to Faraday's constant (96485 C mol^{-1}); C_0 is the concentration of oxygen that has been dissolved in the electrolyte ($1.2 * 10^{-6}$ mol L^{-1}); D_0 by definition, is the diffusion coefficient of oxygen introduced into the electrolyte ($1.9 * 10^{-5}$ cm^2 s^{-1}); ν is the kinetic viscosity of electrolyte (0.01 cm^2 s^{-1}); all constants depend on the electrolyte and in this case refer to 0.1 mol L^{-1} of KOH. After the transformation, the value of the slope of the Koutecky-Levich straight line is obtained, and the number of electrons transferred is calculated on this basis.

Results and Discussion

Materials characterization

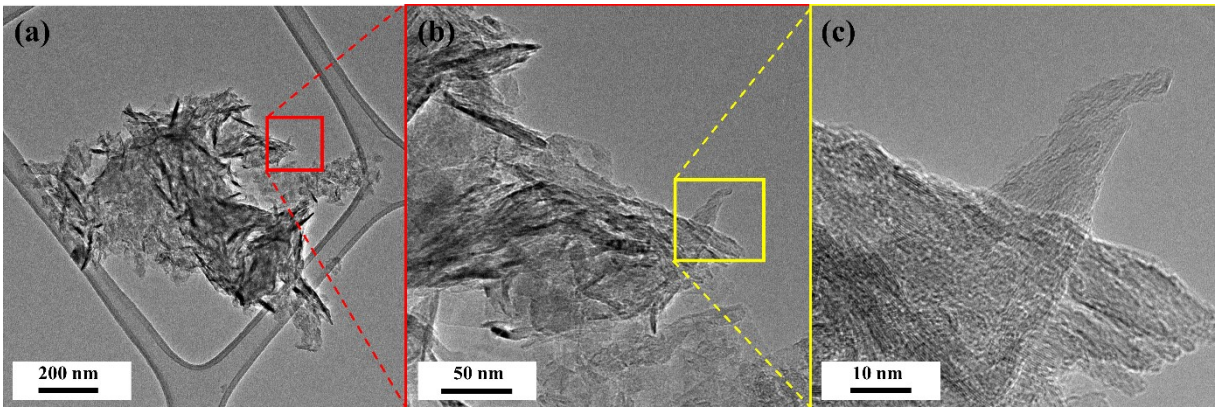

Figure S1. High–resolution transmission electron microscopy images of 2F_800 sample at different magnifications.

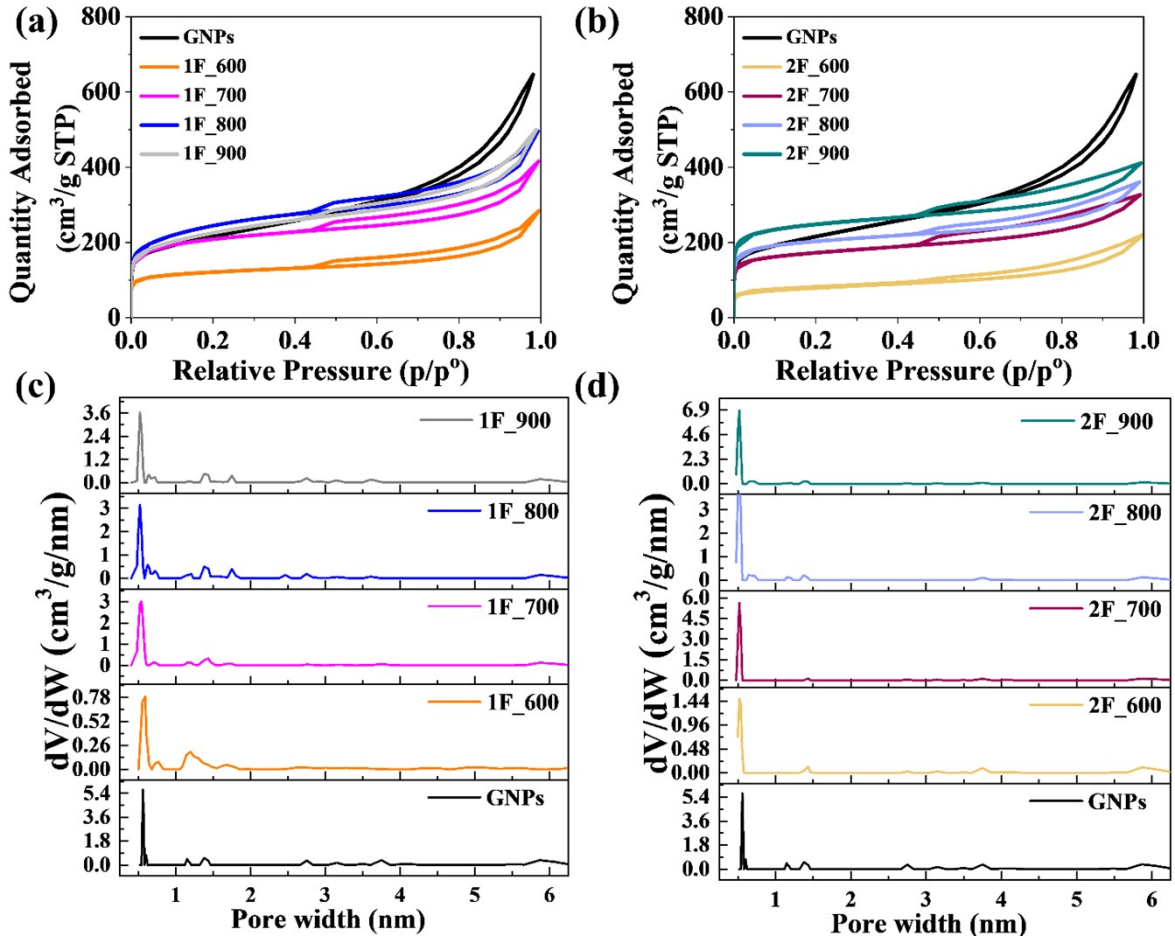

Figure S2. (a, b) Nitrogen adsorption–desorption isotherms and (c, d) pore size distribution of samples in series 1F_T and 2F_T compared with GNPs.

It is noted that the obtained materials do not show significant differences. The pore sizes of the materials obtained in series 1F_T are in the range of micropores (mainly in. 0.51 nm, 0.62 nm, 0.71 nm, 1.37 nm, 1.43 nm, and 1.74 nm) and small mesopores (mainly in 2.36 nm, 2.75 nm, 3.15 nm, 3.61 nm and 5.67 nm). In the case of 2F_T series, the pore size is also in the micropores range (mainly in 0.51 nm, 0.64 nm, 0.71 nm, 1.15 nm, 1.20 nm, 1.37 nm) and small mesopores (mainly in 3.75 nm and 5.87 nm).

The C1s spectrum shows peaks at 284.4 eV, 284.9 eV, 286.2 eV, 287.5eV, 288.6 eV, indicating the presence of C=C (sp^2), C-C (sp^3), C-NH, N-C-O, and O-C=O, respectively (Fig. 3b and Fig. 3f). Deconvolution of the O1s spectrum reveals the presence of O*=C-O and/or O-C-O bonds (530.7eV), and O=C-O* and/or C-O-C type (532.8 eV) (Fig. 3c and Fig. 3g). The N1s spectrum was fitted to four peaks at 398.5 eV, 400.2 eV, 402.3 eV and 404.5 eV, which corresponds to a pyridine-N bond (N-6), a pyrrole-N bond (N-5), quaternary nitrogen (N-Q) and nitrogen oxide $–NO_x$, (N-X), respectively (Fig. 3d and Fig. 3h). In the case of the 2F_800 sample (Fig. 3h), the band located at the binding energy of 404.5 eV is not visible, which means that this type of N-X bonds are not present in this sample.

Table S1. The total amount of C, O, N elements and detailed concentrations for nitrogen-groups determined by XPS analysis of 1F_800 and 2F_800.

Sample	Total C (at. %)	Total O (at. %)	Total N (at. %)	Nitrogen functional group (at. %)				(N-5) and (N-6) (% relative to total N)
				N-5	N-6	N-Q	N-X	
1F_800	93.9	3.5	2.8	1.6	0.7	0.3	0.2	82.14
2F_800	89.9	6.3	3.8	2.3	1.2	0.3	0.0	92.11

Figure 2 presents characteristic bands as D band at ~1350 cm^{-1} that is characteristic of the polycrystalline structure of carbon, which is responsible for doping and defects; a G band at a shift of ~1580 cm^{-1}, characteristic of stretching vibrations in a graphitic crystal. The ratio of D to G bands is usually used to represent defects in the carbon structure. The 2D band at a Raman shift of ~2700 cm^{-1} results from a two-photon process and is the overtone of the D peak [2, 3]. Analyzing the Raman spectra shown in Fig. 2 and comparing the parameters in Table 1, it can be seen that the shape of the D and G bands changes with the carbonization temperature. The area under the D-band is increased for samples carbonized at lower temperatures (1F_600 and 2F_600), indicating that carbon with sp^3 hybridization from chitosan or gelatine was subjected to the elimination of oxygen functional groups by oxidative removal [4]. The G-band responsible for defects in the carbon structure strongly depends on the nitrogen content and is also related to the defective structure. As the carbonization temperature increases, the nitrogen content decreases, and the G-band is more pronounced, indicating that the degree of graphitization increases in all materials obtained [5]. Raman spectroscopy was used to determine the quality of N-doped graphene foams, mainly to estimate how many layers of graphene and determine the defect level of the structure. The calculated intensity ratio of the D to G bands (I_D/I_G) indicates that the structure of the multilayer graphene is defective. A high degree of defectiveness is evidenced by an intensity ratio above or close to the value of 1. The samples obtained in both series show a similar intensity ratio, which may indicate that the samples obtained are equally defective. The observed defective structure is closely related to the heteroatoms that are present in the structure. The intensity ratio of I_D/I_G for samples 1F_600 and 2F_600 was 0.99 and 0.90, respectively. The highest I_D/I_G ratio values for samples 1F_700 and 2F_800 were 1.01 and 1.03, respectively. In both series, the most prominent 2D peak occurs for samples carbonized at 800°C (for 1F_800 and 2F_800), which indicates the presence of graphene structures in the

N-doped graphene foams obtained and also suggests the overlapping of multiple layers. The value of the intensity ratio of the 2D to G bands (I_{2D}/I_G ratio) for all samples is below 0.5 (Table 1) indicate that samples contain the multilayer graphene.

Electrochemical performance

A similar shape and comparable limiting current to the commercial platinum-based carbon material is shown by samples 1F_800 from the first series while for the second series 2F_T, the best shape is shown by samples carbonized at 800°C and 900°C (2F_800 and 2F_900). For the second 2F_T series, the oxygen reduction reaction occurs faster and is more efficient for all samples. This may be related to the respective nitrogen functional groups at the edges of the graphene structures, and more specifically, to the correlation of the N-5 and N-6 groups in relation to the total nitrogen content of the samples. The onset potential values (Table 2) determined from the LSV curves in Fig. 4d and Fig. S3d indicate the rapidity of oxygen reduction on the electrocatalyst. For the 1F_T series synthesized with gelatine, the onset potential values are in the range from 0.83 to 0.87 V vs RHE. The highest value is contained in sample 1F_800, which has an onset potential of 0.87 V vs RHE. The onset potential values for the second series synthesized with chitosan, 2F_T, range from 0.81 to 0.90 V vs RHE, and the highest value is recorded for sample 2F_900 of 0.9 V vs RHE.

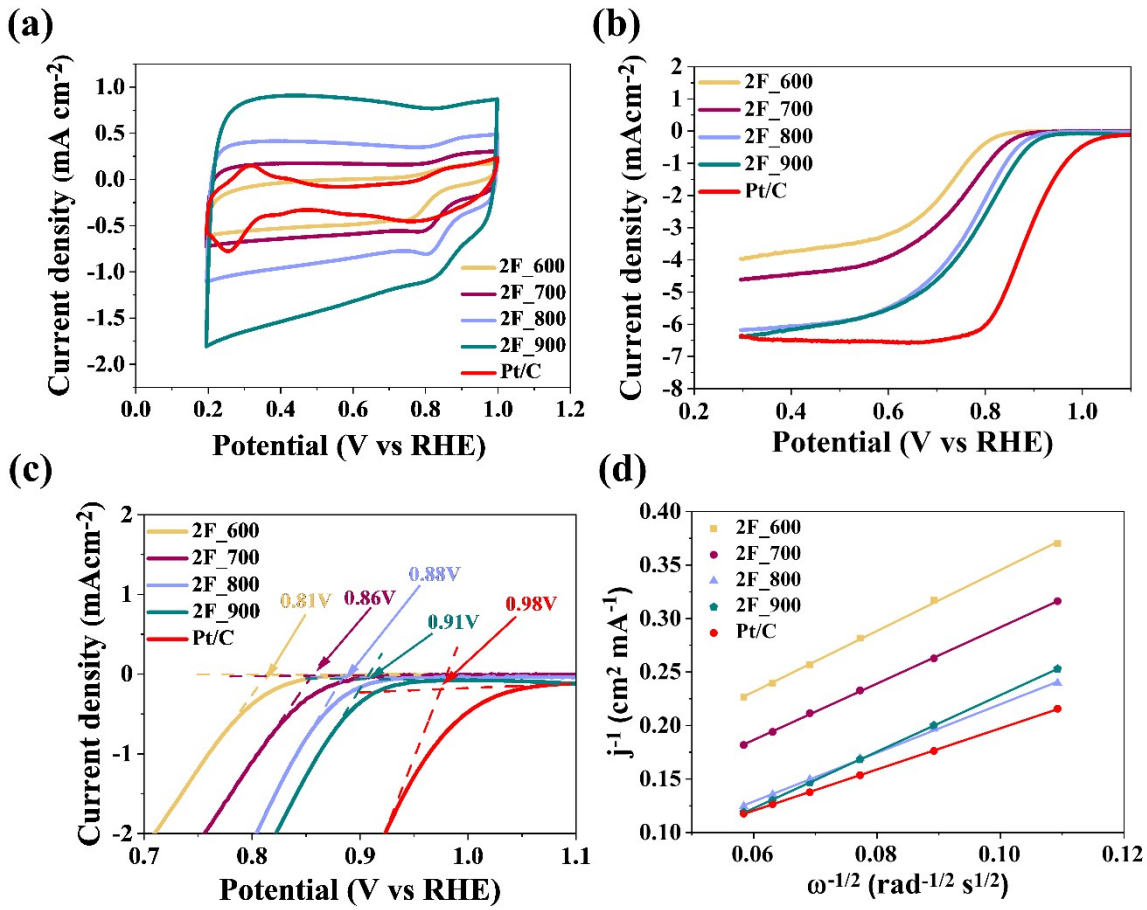

Figure S3. The results of electrochemical performance for 2F_T series and Pt/C in saturated-O_2 0.1 mol L^{-1} KOH (a) CV plots with a scan rate of 10 mV s^{-1}, (b) LSV plots with a scan rate of 5 mV s^{-1} and rotation speed of 1600 rpm, (c) onset potential, (d) Koutecky–Levich plots at 0.5 V vs RHE for samples in the 2F_T series.

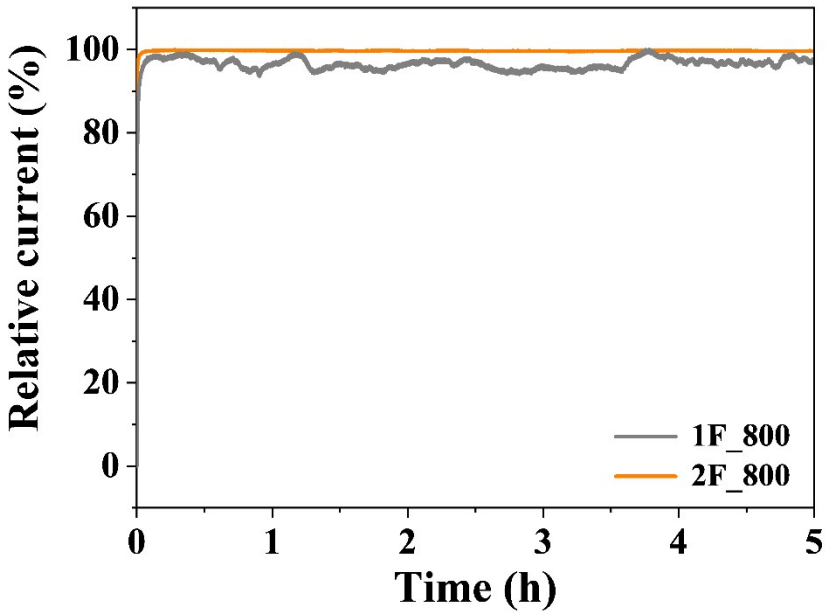

Figure S4. Chronoamperometric curves of 1F_800 and 2F_800 in O_2-saturated 0.1 M KOH solution at 0.5 V vs RHE.

Data availability statement

The datasets generated during and/or analysed during the current study are available in the Open Data Repository - UMK collection https://doi.org/10.18150/9AY0G5.

The datasets used and/or analysed during the current study available from the corresponding author on reasonable request.

References

1. Y. Bian, H. Wang, J. Hu, B. Liu, D. Liu and L. Dai, *Carbon*, 2020, **162**, 66-73.
2. S. A. Chernyak, A. S. Ivanov, D. N. Stolbov, T. B. Egorova, K. I. Maslakov, Z. Shen, V. V. Lunin and S. V. Savilov, *Applied Surface Science*, 2019, **488**, 51-60.
3. A. C. Ferrari and D. M. Basko, *Nature nanotechnology*, 2013, **8**, 235-246.
4. X. Han, M. R. Funk, F. Shen, Y.-C. Chen, Y. Li, C. J. Campbell, J. Dai, X. Yang, J.-W. Kim and Y. Liao, *ACS nano*, 2014, **8**, 8255-8265.
5. G. Mittal, K. Y. Rhee, S. J. Park and D. Hui, *Composites Part B: Engineering*, 2017, **114**, 348-355.